

Identification and monitoring of thiabendazole transformation products in water during Fenton degradation by LC-QTOF-MS

Carla Sirtori · Ana Agüera · Irene Carra ·
José A. Sánchez Pérez

Received: 4 March 2014 / Revised: 21 May 2014 / Accepted: 3 June 2014 / Published online: 20 June 2014
© Springer-Verlag Berlin Heidelberg 2014

Abstract This work enabled the identification of major transformation products (TPs) of thiabendazole (TBZ) during the Fenton process. TBZ is a benzimidazole fungicide widely used around the world to prevent and/or treat a wide range of fruit and vegetable pathogens. The degradation of the parent molecule and the identification of the main TPs were carried out in demineralized water. The TPs were monitored and identified by liquid chromatography-quadrupole time-of-flight mass spectrometry (LC-QTOF-MS/MS). Up to 12 TPs were tentatively identified. Most of them were eliminated after 15 min of treatment time and originated from numerous hydroxylations undergone by the aromatic ring during the initial stages of the process.

Keywords Thiabendazole · Fenton · Transformation products · LC-QTOF-MS/MS

Introduction

A large variety and quantity of pesticides are continuously discharged into the environment worldwide and as such represent a risk for the quality of natural waters. Their application

mainly takes place in agricultural practices, but they are also found in wastewater effluents of food-processing industries including washing steps before crop processing. Although relatively little information exists on pesticide behavior during wastewater treatments, some studies point at the stability of some pesticides in conventional secondary wastewater treatments [1, 2]. An example is the systemic benzimidazole pesticide thiabendazole (TBZ), a widely employed fungicide for pre- and postharvest treatment to control a variety of fruit and vegetable diseases such as mold, blight, rot, and stains caused by various fungi. It is applied by dipping, spraying, or as an ingredient in waxes applied to the skins of fruits and vegetables to ensure freshness [3]. As a consequence of these practices, the presence of TBZ has been reported in river water and sediments [4], bananas, and citrus fruit peel [5, 6] and in the effluent of an agro-food industry, which treats its wastewater with activated sludge in a sequencing batch reactor (SBR) [2]. This and other uses of TBZ in the industry [7, 8] and its reported presence in wastewater [9] necessitate the development of alternative treatments that prevent the contamination of environmental waters from these punctual sources.

Advanced oxidation processes constitute a group of techniques that have received a great deal of attention [10]. They involve “in situ” generation of highly oxidizing species, such as hydroxyl radicals, able to degrade a wide range of organic micropollutants, thus representing an attractive alternative to be used as tertiary treatments [11–13]. In most cases, the efficiency of these treatments is evaluated based on the removal of the target contaminants or by global parameters, but an important issue is the formation of transformation products (TPs) during these processes. These TPs can lead to an increase in the toxicity of the treated water and, in many cases, are more resistant to degradation [14]. Thus, optimization of water treatments must also consider the formation/degradation of these degradation intermediates to ensure the quality of the treated water, especially if they are intended for reuse [15]. In

C. Sirtori (✉)
Instituto de Química/UFRGS, Av. Bento Gonçalves, 9500, Bairro:
Agronomia, Porto Alegre, RS 91509-900, Brazil
e-mail: carla.sirtori@ufrgs.br

A. Agüera
Department of Chemistry and Physics, University of Almería, La
Cañada de San Urbano, 04120 Almería, Spain

A. Agüera · I. Carra · J. A. Sánchez Pérez
CIESOL, Joint Centre of the University of Almería-CIEMAT, La
Cañada de San Urbano, 04120 Almería, Spain

I. Carra · J. A. Sánchez Pérez
Department of Chemical Engineering, University of Almería, La
Cañada de San Urbano, 04120 Almería, Spain

addition, TPs generated during the oxidative treatments may be reasonably similar to those actually occurring in the environment [16], thus further justifying the interest in TP identification studies.

However, these studies face serious difficulties, which represent a challenge for analytical researchers. The variety in structures and polarities, low concentrations, and the absence of analytical standards make the accurate assignment of structures difficult, which is only possible by using analytical tools such as gas chromatography (GC) or liquid chromatography (LC) in combination with mass spectrometry (MS) [17]. The use of triple quadrupole (QqQ) systems provides valuable structural information by performing tandem mass (MS/MS) experiments, which increase the fragmentation of selected precursor ions [18]. The application of ion trap mass analyzers, able to perform multiple-stage (MSⁿ) experiments, also represents an improvement in the identification capability of LC- and GC-MS instruments. Thus, selected ion fragments obtained at the first stage of analysis can be further selected, isolated, and fragmented to increase the possibility of confirming the proposed structures [19]. However, in the last decade, high-resolution mass spectrometry (HRMS) has become the most popular option for the identification of unknown TPs. Time-of-flight (TOF) and OrbitrapTM instruments and their hybrid configurations, quadrupole time-of-flight (QTOF), ion trap-Orbitrap (LTQOrbitrapTM), or quadrupole-Orbitrap (Q ExactiveTM) mass spectrometers, generally in combination with API-liquid chromatography, have been widely applied for this purpose [20]. The ability of accurate mass measurements with these instruments allows elemental compositions of unknown molecules to be achieved, with mass errors in the low ppm range or lower, thus reducing the list of possible formulas and providing a high grade of certainty in their assignment.

In this work, the application of liquid chromatography-quadrupole time-of-flight mass spectrometry (LC-QTOF-MS) has been studied to identify the major TPs resulting from TBZ resulting from degradation in water by the Fenton process. Some previous attempts have been made to identify degradation intermediates of TBZ generated by other processes, such as UV [21, 22] or TiO₂ photocatalysis [23]. A previous work carried out by our group reported the degradation of TBZ by the Fenton process, identifying major TPs [2], but this is the first time that a comprehensive study has evaluated the transformation route of this compound by the Fenton process. To our knowledge, high-resolution mass spectrometry has not been previously applied for this purpose. The use of QTOF-MS/MS has provided analytical information useful for a more reliable structure assignment, thus improving the existing information and allowing identification of new unreported TPs. The main transformation mechanisms have been described and a tentative degradation pathway proposed, therefore increasing the available knowledge about the behavior of this compound.

Experimental

Chemicals

Thiabendazole (2-(4-thiazolyl)benzimidazole; 99 %), benzimidazole, and thiazol-4-carboxamide (98 %) were purchased from Sigma-Aldrich. For chromatographic analysis, high-performance liquid chromatography (HPLC)-grade methanol supplied by Merck (Germany), Milli-Q ultra-pure water system from Millipore (Milford, MA, USA), and formic acid (purity, 98 %) from Fluka were used. All Fenton experiments were performed using iron sulfate heptahydrate (FeSO₄ 7H₂O), reagent-grade hydrogen peroxide (30 % w/v), and sulfuric acid (97–98 %) for pH adjustment, all purchased from Panreac.

Experimental setup

The Fenton process was performed in a magnetically stirred glass vessel (5 L). TBZ degradation was evaluated in demineralized water, and the initial concentration was 20 mg L⁻¹. During the reaction, the system was protected from light. The pH was adjusted to 2.8 (H₂SO₄, 2 N). Initial hydrogen peroxide concentration was 100 mg L⁻¹. The catalyst (iron) was dosed every 5 min in increasing amounts as FeSO₄ 7H₂O solution. The iron sequence applied was 5, 5, 5, 10, and 20 mg L⁻¹. This strategy was followed to ensure slow degradation at first so that as many TPs as possible could be detected and high TBZ degradation could ultimately be achieved.

Analytical determinations

The total iron concentration was determined according to the *o*-phenantroline standardized procedure (ISO 6332), and the red complex formed was determined spectrophotometrically at 510 nm. Hydrogen peroxide was analyzed by a quick, simple spectrophotometric method using ammonium metavanadate, which allows the H₂O₂ concentration to be calculated instantaneously based on a red-orange peroxovanadium cation formed during the reaction of H₂O₂ with metavanadate, the maximum absorption of which is at 450 nm. The peroxide concentrations are calculated from absorption measurements by a ratio found by Nogueira et al. [24].

TPs generated during the Fenton process were monitored by LC-QTOF-MS/MS. The chromatographic system was equipped with a SB-C18 analytical column of 3.0 mm × 250 mm, 5 μm of particle size (Agilent Technologies); 0.1 % formic acid and 5 % Milli-Q water in acetonitrile were used as mobile phase A and 0.1 % formic acid in water (pH 3.5) as mobile phase B. The elution gradient went from 10 % A (3 min) to 100 % A in 22 min and was kept thereafter

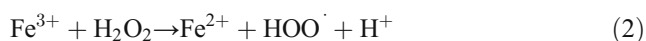
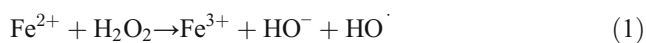
at 100 % A for 3 min. The flow rate was 0.5 mL min⁻¹ and the injection volume, 10 µL. The HPLC system was connected to a quadrupole time-of-flight mass spectrometer (Agilent 6530 Q-TOF MS, Agilent Technologies, Santa Clara, CA). The instrument was operated in the 4-GHz high-resolution mode. Ions were generated using an electrospray ion source with Agilent Jet Stream Technology. The operating conditions were as follows: superheated nitrogen sheath gas temperature, 400 °C at a flow rate of 12 L min⁻¹; nozzle voltage, 0 V; capillary, 4,000 V; nebulizer, 60 psi; drying gas, 5 L min⁻¹; gas temperature, 250 °C; skimmer voltage, 65 V; octapole RF Peak, 750 V; and fragment or (in source CID fragmentation), 90 V. MS/MS spectra were acquired throughout the *m/z* 40–950 range at a scan rate of 0.5 s/spectrum. The collision energy was optimized to obtain the highest number of fragments. The full mass spectra data recorded were processed with Agilent Mass Hunter Workstation Software (version B.03.01).

Results and discussion

Thiabendazole degradation by the Fenton treatment

The Fenton process belongs to the group of well-known advanced oxidation processes (AOPs). This treatment is often used to remove organic persistent pollutants [25] and is initiated by the reaction of ferrous iron with hydrogen peroxide to yield hydroxyl radicals (reaction 1). Ferric iron subsequently reacts again with hydrogen peroxide, yielding perhydroxyl radicals (reaction 2). The process is catalyzed by iron and uses hydrogen peroxide as reactant.

Both radicals, hydroxyl and perhydroxyl, are oxidant species which react with the pollutants, in this case TBZ, to generate TPs (reactions 3 and 4). However, hydroxyl radicals are more oxidant than perhydroxyl radicals, so the oxidation is mainly due to the former [26].



As such, the Fenton process was applied in order to degrade TBZ at a concentration of 20 mg L⁻¹ in a demineralized water solution. Iron was added in increasing additions up to a

total concentration of 45 mg L⁻¹, as described in the “Experimental” section. Hydrogen peroxide was used in excess (100 mg L⁻¹) to guarantee that there was no lack of oxidant. The sequential iron dosage ensured slow TBZ degradation and, consequently, the detection of more TPs, but also a high final degradation.

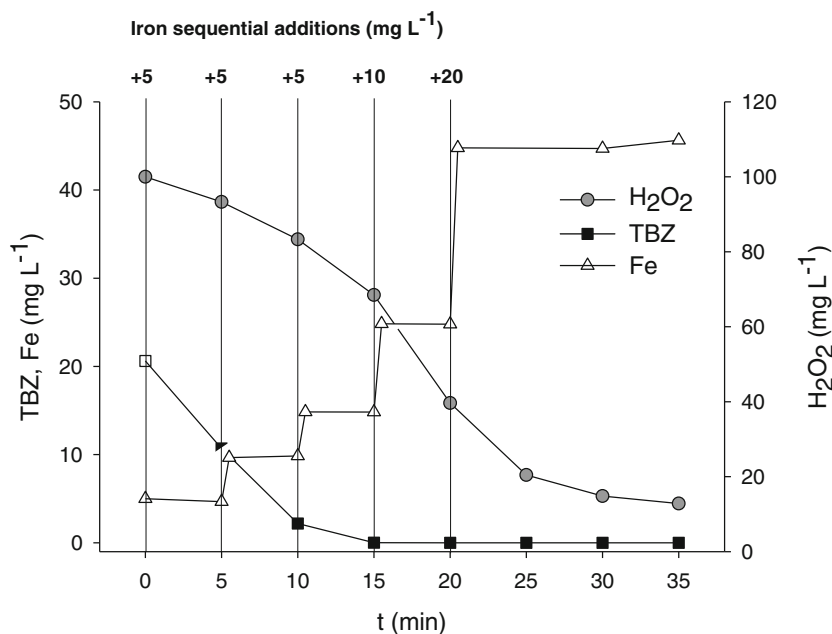
Figure 1 shows the results obtained throughout the Fenton process. Total elimination of TBZ was obtained after the last iron addition (45 mg L⁻¹), although 99 % degradation had already been achieved with 25 mg L⁻¹ of iron dosage. At this point, 60 mg L⁻¹ H₂O₂ had been consumed, so the oxidant was not limiting the reaction.

Identification of TPs by LC-QTOF-MS/MS

Tentative identification of TPs generated during the Fenton treatment of TBZ in aqueous solution was undertaken by using an LC-QTOF-MS system operated in ESI (+) mode. Water samples were taken after each iron addition (5, 10, 15, 20, and 25 min) and at the end of the experiment (35 min), which corresponds with the concentrations of TBZ shown in Fig. 1. Analyses in scan mode allowed the appearance-disappearance of peaks (was indicative of possible TPs) to be monitored. The total ion chromatogram acquired after the second iron addition (10 min of treatment) and the extracted ion chromatograms corresponding with the TPs detected are shown in Fig. 2. Elemental compositions of protonated molecules, included in Table 1, were provided by the software with a score higher than 98 % in all cases. These score values are based on how the mass and the isotope pattern calculated from the formula match the measured values. The high values obtained provide a high degree of certainty for the proposed formulae. However, structural elucidation required additional information, which was obtained by MS/MS analyses. MS/MS spectra of the suspected peaks were registered to obtain the maximum number of fragment ions useful for confirmation purposes. Figures 3, 4, 5, and 6 show the mass spectra of TBZ and TPs identified as well as tentative structures of some relevant ion fragments. Table 1 displays analytical information corresponding to the compounds identified, such as retention time, elemental composition of the protonated molecules [M+H]⁺ and product ions, the experimental exact masses, the difference between the observed and calculated *m/z* (in parts per million), and information concerning the degree of unsaturation of the molecules (double bond equivalents (DBE)).

As a preliminary step, an interpretation of the product ion spectrum of TBZ was proposed since the fragmentation pattern of the parent compound is often useful in the interpretation of mass spectra of the TPs. The occurrence of typical losses and presence/absence of characteristic fragment ions can provide valuable information about the transformations undergone by the TBZ molecule. Therefore, the protonated

Fig. 1 TBZ degradation and iron (II) and H₂O₂ consumption during the Fenton treatment in demineralized water



molecule of TBZ (C₁₀H₈N₃S, *m/z* 202.0433) displayed a rich product ion spectrum with fragments at *m/z* 175, 143, 131, 104, 92, 77, and 65 (expressed as nominal mass). The structure of the two major ions (*m/z* 175 and *m/z* 131) has previously been proposed by Calza et al. [23]. The ion at *m/z* 175 is generated by the neutral loss of HCN (27 Da) with consequent opening of the thiazole ring. Further loss of CS (44 Da) yields the fragment at *m/z* 131. Other typical fragments are shown in Fig. 3a. C₉H₇N₂ (*m/z* 143) fragment ion is produced by loss of S from the ion at *m/z* 175. This fragment is a precursor of *m/z* 131, which undergoes an extra new loss of HCN to yield C₇H₆N (*m/z* 104). Other less specific fragments correspond to the ions C₆H₆N (*m/z* 92), C₆H₅ (*m/z* 77), and C₅H₅ (*m/z* 65) which are characteristic of the phenyl moiety.

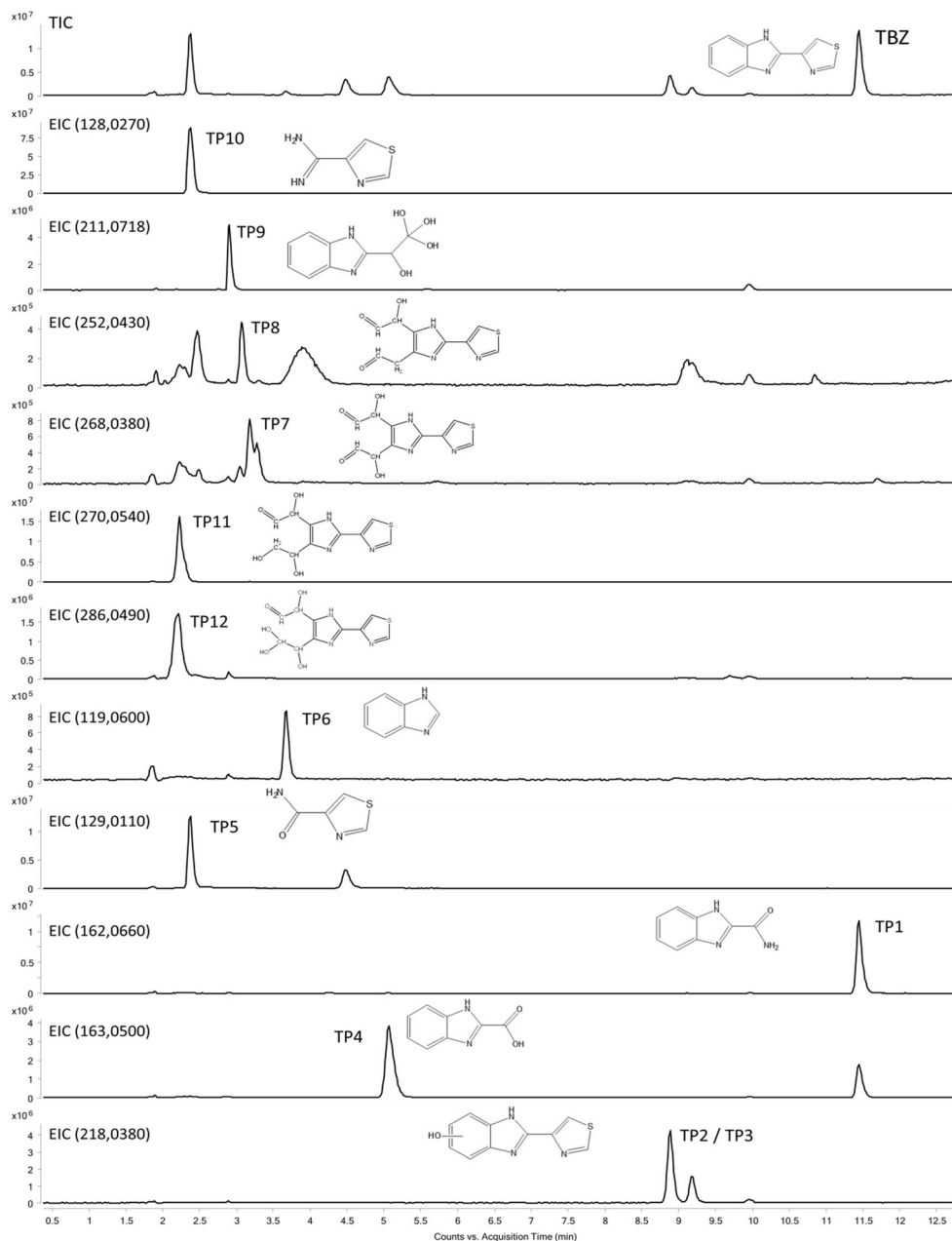
The molecular ions of TP2 and TP3 showed the same *m/z* and elemental composition (C₁₀H₈N₃SO, *m/z* 218.0387), but including in this case an extra oxygen atom with respect to the formula of TBZ. Thus, the formula was consistent with monohydroxylated products of TBZ, generated by an attack of the OH radicals on different positions of the molecule. These reactions are quite common in advanced oxidation processes, and due to the nonselective nature of these oxidative species, multiple positional isomers of mono-, di-, and even trihydroxylated TPs are frequently detected [27]. However, differentiation of these isomers is not always feasible by LC-MS. In our study, accurate mass spectra obtained for both compounds did not exhibit significant differences, and the exact assignment of the hydroxylation position for TP2 and TP3 could not be proposed. Both isomers showed the same fragmentation pattern as TBZ, with common mass fragments at *m/z* 191 (C₉H₇N₂OS), 159 (C₉H₇N₂O), and 147 (C₈H₇N₂O). However, the presence of the oxygen atom in

these fragments confirmed the position of the OH group in the benzimidazole moiety (Fig. 3b). This conclusion is also supported by the known electrophilic nature of the hydroxyl radicals and the rich electron density of benzimidazole ring, which may facilitate its addition. The loss of a water molecule, indicative of the presence of an alcoholic group, was also detected (*m/z* 173, C₉H₅N₂S), thus confirming the proposed structure. The similarity between TP2 and TP3 spectra suggests that the OH occupies similar positions in the benzene ring. This concurs with the reported formation of 5-hydroxythiabenzazole (5-hydroxy-2-(4-thiazolyl)benzimidazole) as part of human metabolism [28].

TP1 yielded an *m/z* ratio of 162.0662 (C₈H₈N₃O), which is consistent with the photoproduct previously identified by Murthy et al. [22] as benzimidazole-2-carboximide. In this case, identification of the TPs, generated by irradiation under UV light, was performed by GC-MS. However, the fragmentation observed for benzimidazole-2-carboximide coincides with that obtained for TP1 in our study (Fig. 3c). The fragment at *m/z* 145, which shows the formula C₈H₅N₂O, was associated with the neutral loss of NH₃ (17 Da), while the ion at *m/z* 117 (C₇H₅N₂) corresponded to a neutral loss of 28 Da, which was assigned to the output of the CO group. Finally, fragments at *m/z* 90 (C₆H₄N) and 63 (C₅H₃) coincided with two successive losses of HCN.

TP4 (*m/z* 163.0502, C₈H₇N₂O₂) was assigned as 1H-benzo[d]imidazole-2-carboxylic acid, which to our knowledge, had not been previously reported in the literature. This TP was generated by substitution of the amine group in TP1 by hydroxyl radicals, leading to the oxidation of the molecule and formation of the acidic derivative. Because of the similarity of the structures, the accurate mass spectrum of TP4

Fig. 2 Total ion chromatogram acquired after the second iron addition (10 min of treatment) and extracted ion chromatograms corresponding to the TPs detected



showed the same product ion profile as TP1, but in this case, the fragments at m/z 145 and m/z 117 arose from stepwise elimination of H_2O and CO , pointing to the presence of the carboxylic group (Fig. 4a).

The MS/MS spectrum of TP6 (m/z 119.0603, $\text{C}_7\text{H}_7\text{N}_2$) was consistent with benzimidazole structure (Fig. 4b). The fragmentation route of this compound was characterized by two consecutive losses of HCN , related to the presence of two nitrogen atoms in the imidazole ring, which yielded fragment ions at m/z 92.0495 ($\text{C}_6\text{H}_6\text{N}$) and 65.0390 (C_5H_5). The identity of this TP was compared with that of previous literature [2, 22, 23] and was unequivocally confirmed by analysis of the commercial standard.

The best-fit formula for TP9 (m/z 211.0718) was $\text{C}_9\text{H}_{11}\text{N}_2\text{O}_4$. The absence of sulfur in the molecule and the decrease of the DBE value by three units with respect to TBZ were indicative of a breakage of the thiazole ring, associated with the loss of N, S, and C. Furthermore, the molecule contained four additional oxygen atoms, indicating a high degree of oxidation. Observation of the MS/MS spectrum (Fig. 4c) allowed us to confirm that part of it was identical to the spectrum of benzimidazole (fragments at m/z 119, 92, and 65), thus indicating the integrity of this part of the molecule. Consequently, oxygen atoms were located in the aliphatic chain as alcoholic functionalities, according to a DBE value of 6. Successive losses of H_2O and CO observed in the mass

Table 1 Accurate mass measurements obtained by LC-QTOF-MS/MS for TBZ and TPs generated during the Fenton treatment

| | t_r | Ion formula $[M+H]^+$ | Experimental mass | Error (ppm) | DBE |
|--------------------|-----------|-----------------------|-------------------|-----------------------|----------|
| TBZ | 9.92 | $C_{10}H_8N_3S$ | 202.0437 | -1.58 | 9 |
| | | $C_9H_7N_2S$ | 175.0326 | -0.79 | 7.5 |
| | | $C_9H_7N_2$ | 143.0604 | 1.17 | 7.5 |
| | | $C_8H_7N_2$ | 131.0604 | 0.03 | 6.5 |
| | | C_7H_6N | 104.0492 | 2.3 | 5.5 |
| | | C_6H_6N | 92.0495 | -0.08 | 4.5 |
| | | C_6H_5 | 77.0393 | -8.79 | 4.5 |
| | | C_5H_5 | 65.0389 | -5.13 | 3.5 |
| TP1 | 11.39 | $C_8H_8N_3O$ | 162.0662 | -1.92 | 7 |
| | | $C_8H_5N_2O$ | 145.0394 | 1.7 | 7.5 |
| | | $C_7H_5N_2$ | 117.0445 | 6.24 | 6.5 |
| | | C_6H_4N | 90.0342 | -4.44 | 5.5 |
| | | C_5H_3 | 63.0227 | -4.75 | 4.5 |
| TP2/TP3 | 8.88/9.17 | $C_{10}H_8N_3OS$ | 218.0387 | 0.17 | 9 |
| | | $C_9H_7N_2OS$ | 191.0278 | -2.13 | 7.5 |
| | | $C_9H_5N_2S$ | 173.0160 | 8.96 | 8.5 |
| | | $C_9H_7N_2O$ | 159.0556 | -1.78 | 7.5 |
| | | $C_8H_7N_2O$ | 147.0554 | -0.83 | 6.5 |
| | | $C_4H_3N_2S$ | 111.0003 | 8.06 | 4.5 |
| | | C_5H_6N | 80.0489 | 7.16 | 3.5 |
| | | $C_8H_7N_2O_2$ | 163.0502 | -0.03 | 7 |
| TP4 | 5.06 | $C_8H_5N_2O$ | 145.0394 | 1.96 | 7.5 |
| | | $C_7H_5N_2$ | 117.0441 | 3.88 | 6.5 |
| | | C_6H_4N | 90.0341 | -0.99 | 5.5 |
| | | C_5H_3 | 63.0227 | -4.75 | 4.5 |
| | | $C_4H_3N_2OS$ | 129.0118 | -0.09 | 4 |
| TP5 | 4.48 | C_4H_2NOS | 111.985 | 2.02 | 4.5 |
| | | C_3H_2NS | 83.9907 | -3.84 | 3.5 |
| | | C_2HS | 56.9799 | -7.60 | 2.5 |
| | | $C_7H_7N_2$ | 119.0603 | -0.19 | 6 |
| TP6 | 3.66 | C_6H_6N | 92.0495 | -0.06 | 4.5 |
| | | C_5H_5 | 65.039 | -6.55 | 3.5 |
| | | $C_{10}H_{10}N_3O_4S$ | 268.0384 | 1.02 | 7.5 |
| TP7 | 3.16 | $C_{10}H_8N_3O_3S$ | 250.0243 | 15.23 | 8.5 |
| | | $C_{10}H_6N_3O_2S$ | 232.0169 | 2.68 | 9.5 |
| | | $C_9H_8N_3O_2S$ | 222.0317 | 6.72 | 7.5 |
| | | $C_9H_6N_3OS$ | 204.0227 | -0.52 | 8.5 |
| | | $C_8H_8N_3OS$ | 194.036 | 11.65 | 6.5 |
| | | $C_7H_8N_3S$ | 166.0435 | -0.79 | 5.5 |
| | | $C_7H_5N_2S$ | 149.0163 | 3.1 | 6.5 |
| | | C_6H_4NS | 122.0054 | 3.86 | 5.5 |
| | | $C_4H_3N_2S$ | 111.0011 | -1.86 | 4.5 |
| | | $C_6H_5N_2$ | 105.0451 | -3.11 | 5.5 |
| | | C_3H_2NS | 83.9899 | 3.4 | 3.5 |
| | | C_3H_6N | 56.0501 | -11.62 | 1.5 |
| | | TP8 | 3.08 | $C_{10}H_{10}N_3O_3S$ | 252.0438 |
| $C_{10}H_8N_3O_2S$ | 234.0299 | | | 13.78 | 8.5 |
| $C_9H_8N_3OS$ | 206.0353 | | | 14.93 | 7.5 |
| $C_8H_8N_3S$ | 178.0433 | | | -5.74 | 6.5 |

Table 1 (continued)

| | t_r | Ion formula [M+H] ⁺ | Experimental mass | Error (ppm) | DBE |
|------|-------|---|-------------------|-------------|-----|
| TP9 | 2.90 | C ₈ H ₆ NO ₃ | 164.0328 | 8.49 | 6.5 |
| | | C ₄ H ₃ N ₂ S | 111.0003 | 8.06 | 4.5 |
| | | C ₆ H ₄ NO | 106.0286 | 0.87 | 5.5 |
| | | C ₄ H ₆ N | 68.0495 | 0.29 | 2.5 |
| | | C ₉ H ₁₁ N ₂ O ₄ | 211.0718 | -2.3 | 6 |
| | | C ₉ H ₇ N ₂ O ₂ | 175.0495 | 3.17 | 7.5 |
| | | C ₈ H ₇ N ₂ O | 147.0545 | 2.76 | 6.5 |
| | | C ₇ H ₇ N ₂ | 119.0601 | 1.84 | 5.5 |
| | | C ₆ H ₆ N | 92.0489 | 6.21 | 4.5 |
| TP10 | 2.38 | C ₅ H ₅ | 65.039 | -6.55 | 3.5 |
| | | C ₄ H ₆ N ₃ S | 128.0279 | 1.14 | 3.5 |
| | | C ₄ H ₃ N ₂ S | 111.0009 | 2.34 | 4.5 |
| | | C ₃ H ₂ NS | 83.9902 | -1.19 | 3.5 |
| TP11 | 2.18 | C ₂ HS | 56.9798 | -7.56 | 2.5 |
| | | C ₁₀ H ₁₂ N ₃ O ₄ S | 270.0546 | -2.05 | 7 |
| | | C ₁₀ H ₁₀ N ₃ O ₃ S | 252.0433 | 1.26 | 7.5 |
| | | C ₁₀ H ₈ N ₃ O ₂ S | 234.0334 | -1.29 | 8.5 |
| | | C ₉ H ₈ N ₃ OS | 206.0382 | -0.46 | 7.5 |
| | | C ₈ H ₈ N ₃ S | 178.0431 | 1.74 | 6.5 |
| | | C ₇ H ₇ N ₃ S | 165.0349 | 0.91 | 6 |
| | | C ₈ H ₉ NO ₂ | 151.0613 | 0.91 | 5 |
| | | C ₄ H ₃ N ₂ S | 111.001 | -0.82 | 4.5 |
| TP12 | 2.13 | C ₅ H ₆ NO | 96.0443 | 2.03 | 3.5 |
| | | C ₁₀ H ₁₂ N ₃ O ₃ S | 286.0493 | 0.66 | 7 |
| | | C ₁₀ H ₁₀ N ₃ O ₄ S | 268.0394 | 1.55 | 7.5 |
| | | C ₁₀ H ₈ N ₃ O ₃ S | 250.0282 | 1.82 | 8.5 |
| | | C ₁₀ H ₆ N ₃ O ₂ S | 232.0168 | 2.85 | 9.5 |
| | | C ₉ H ₈ N ₃ O ₂ S | 222.033 | 5.72 | 7.5 |
| | | C ₉ H ₆ N ₃ OS | 204.0246 | -7.76 | 8.5 |
| | | C ₈ H ₈ N ₃ OS | 194.0384 | 5.78 | 6.5 |
| | | C ₈ H ₅ N ₂ OS | 177.0126 | -1.9 | 7.5 |
| | | C ₈ H ₉ N ₂ O ₂ | 165.0662 | -2.02 | 5.5 |
| | | C ₄ H ₆ N ₃ S | 128.0287 | -2.44 | 3.5 |
| | | C ₄ H ₃ N ₂ S | 111.001 | 0.44 | 4.5 |
| | | C ₆ H ₅ N ₂ | 105.0453 | -5.16 | 5.5 |

spectrum are consistent with this hypothesis. Based on these observations, TP9 was tentatively identified as 1-(1H-benzo[d]imidazol-2-yl)ethane-1,2,2,2-tetraol. To our knowledge, identification of TP9 is the first evidence reported of the attack of hydroxyl radicals on the thiazole ring.

TP5 (m/z 129.0118, C₄H₅N₂OS) and TP10 (m/z 128.0279, C₄H₆N₃S) showed a very similar fragmentation profile with characteristic fragments at m/z 111, 83.9, and 57 (Fig. 5a, b). However, while the two last fragments corresponded with the same formula, accurate mass measurements allowed for differentiation between fragments at m/z 111.985 (C₄H₂NOS) for TP5 and m/z

111.0009 (C₄H₃N₂S) for TP10. Fragmentation of TP10 was attributed to a loss of NH₃ and two consecutive losses of HCN. TP5 yielded fragments corresponding with successive losses of NH₃, CO, and HCN. This fragmentation was similar to that obtained by GC-EIMS by Murthy et al. [22] and assigned to thiazole-4-carboxamide. The availability of the commercial standard allowed the unambiguous confirmation of this intermediate confirmation. TP10 was identified as thiazole-4-carboximidine and could possibly correspond with a previous step in the oxidation of TBZ molecule after the benzimidazol ring opening.

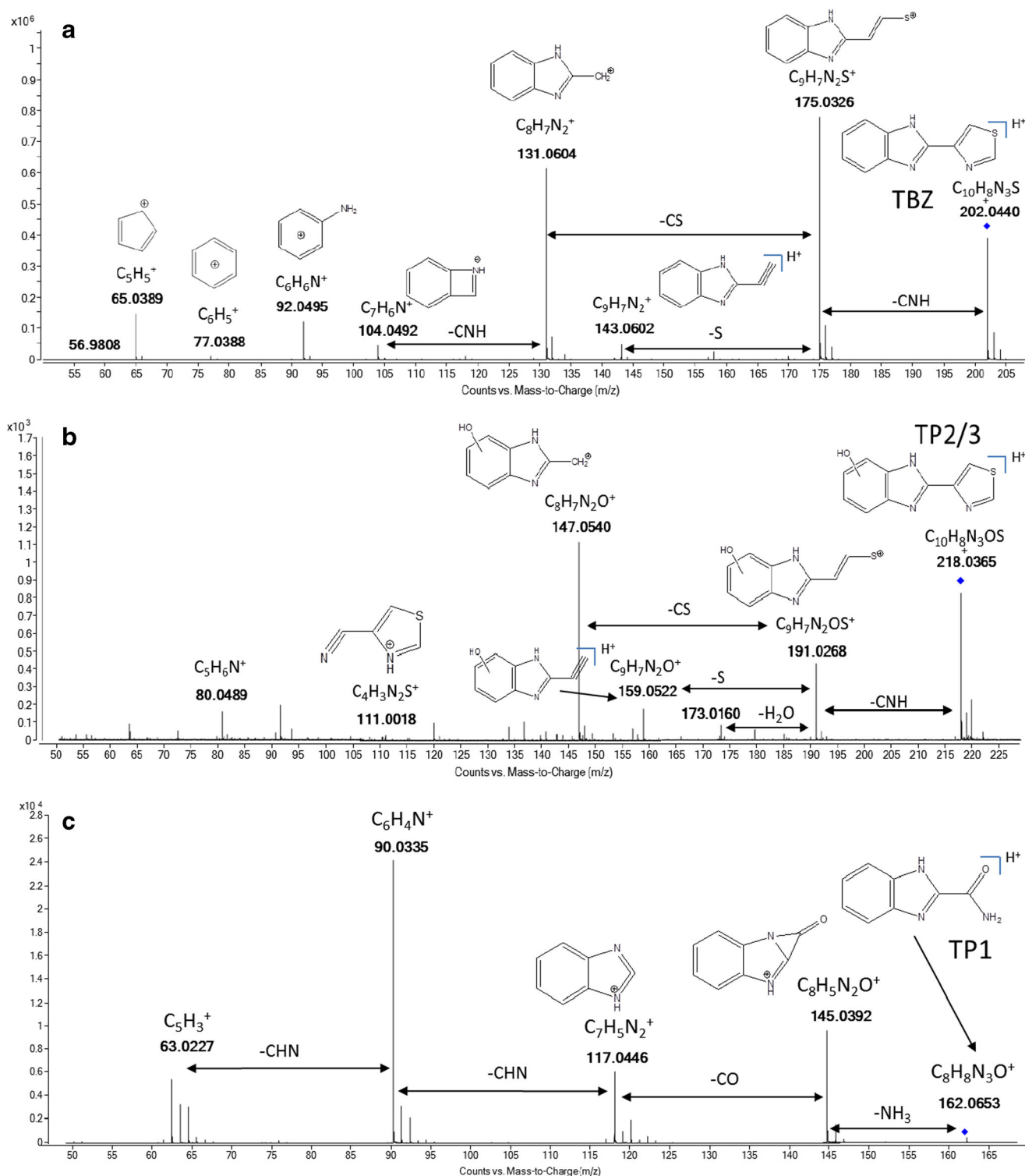


Fig. 3 Product ion spectra of TBZ (a), TP2/3 (b), and TP1 (c) obtained by LC-QTOF-MS/MS and tentative fragment ion structures

TP7, TP8, TP11, and TP12 were identified as potential products of the cleavage of the benzene ring by the attack of multiple OH radicals on the C1–C2 double bond. This reaction can be considered to be the next step in the hydroxylation reaction already described in TP2 and TP3, which leads to the

subsequent ring opening. Calza et al. [23] reported this route as a potential TiO_2 -induced photodegradation pathway of TBZ through identification of TP7 and TP11. In our study, this route has been confirmed by the identification of two new compounds, TP8 and TP12.

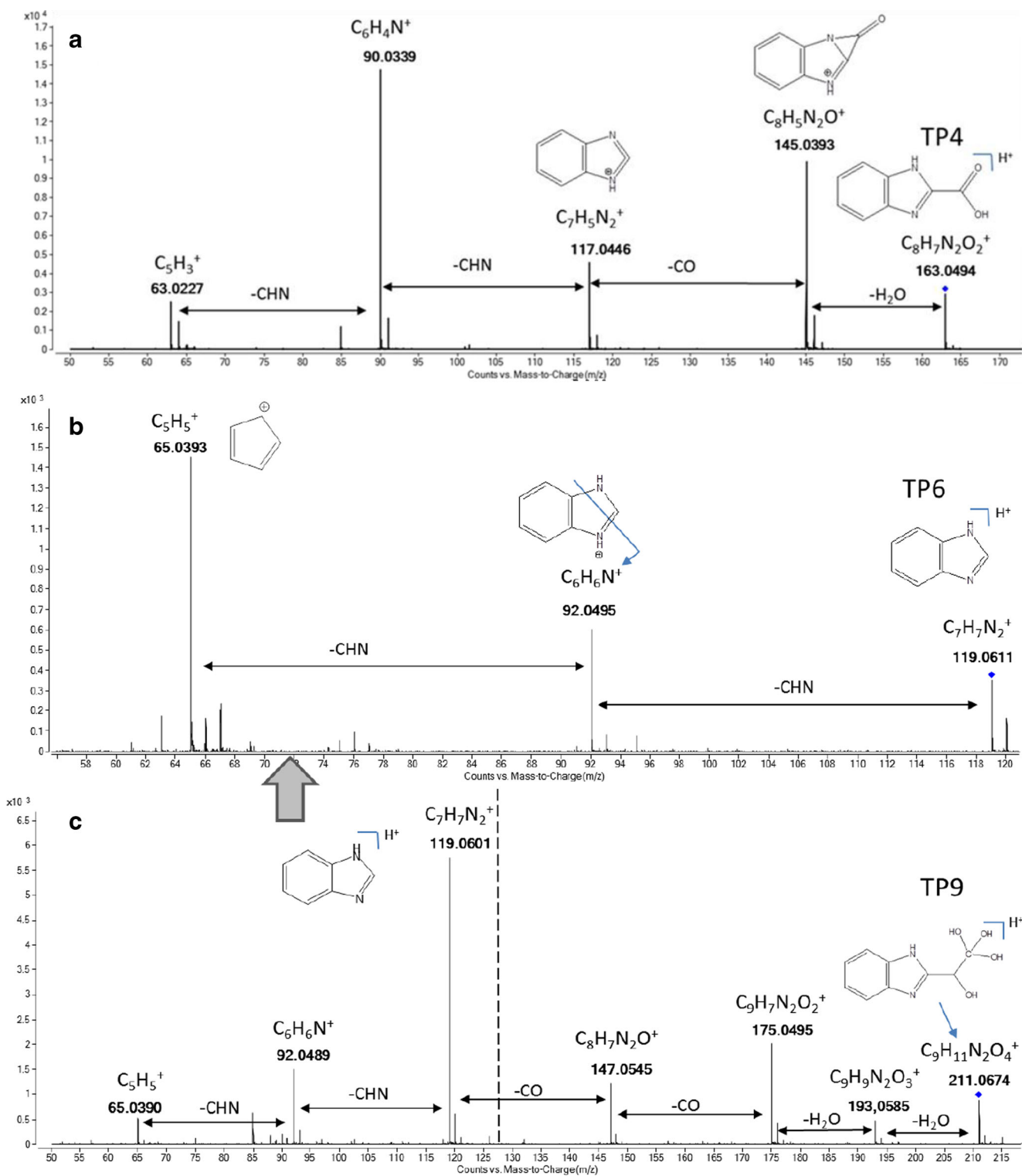


Fig. 4 Product ion spectra of TP4 (a), TP6 (b), and TP9 (c) obtained by LC-QTOF-MS/MS and tentative fragment ion structures

TP11 (m/z 270.0540, $C_{10}H_{12}N_3O_4S$) showed a mass spectrum with abundant fragmentation (Fig. 5c). DBE was reduced by two units with respect to TBZ, indicating that the benzene ring opening was accompanied by the reduction of double bonds by OH radicals. Some of the

observed ions (m/z 252, 234, 224, and 206) were common to those reported by Calza et al. [23], carried out in an ion trap mass spectrometer using multiple-stage (MS^2 and MS^3) experiments. These fragments corresponded with two successive losses of water CO , typically attributed

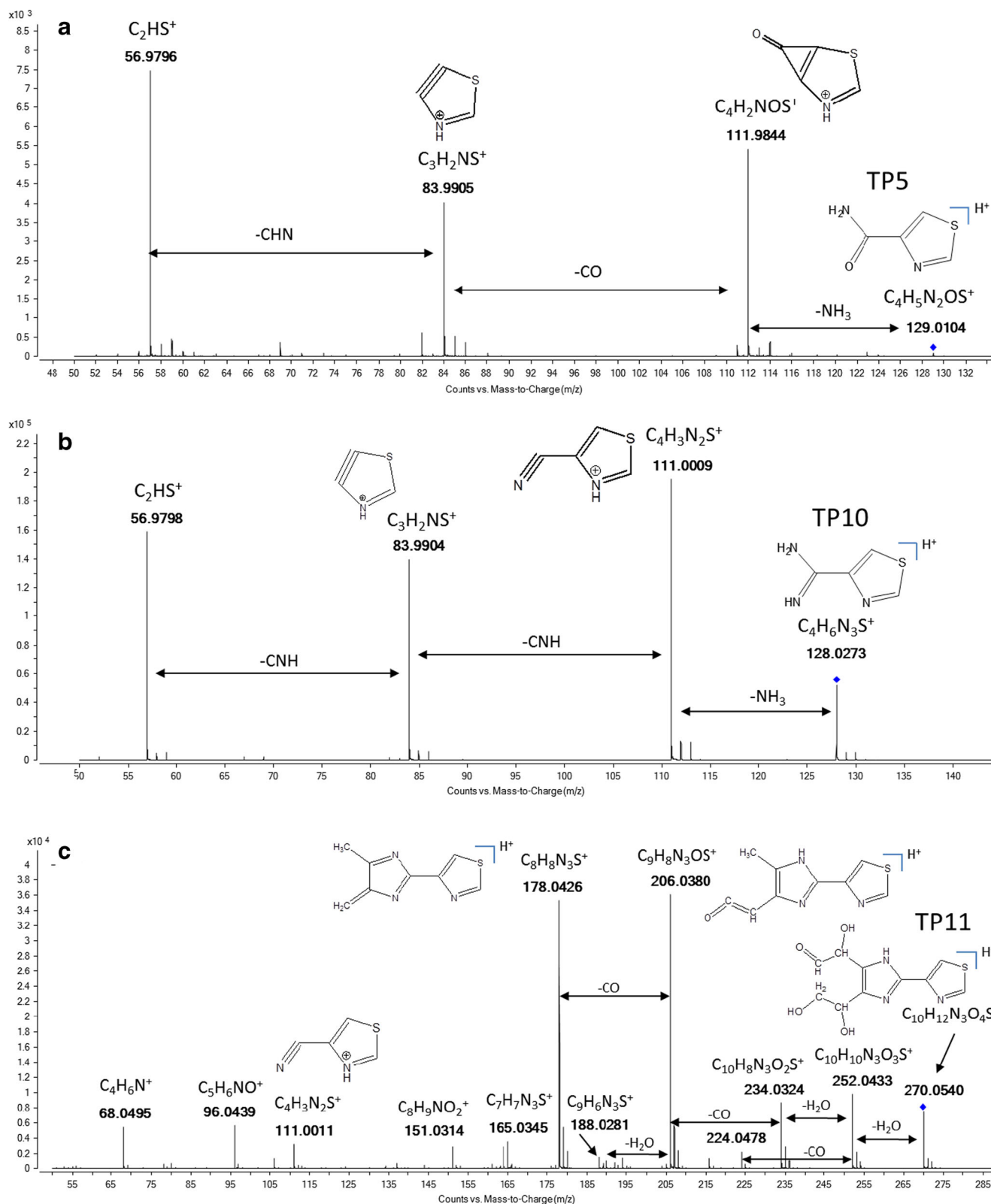


Fig. 5 Product ion spectra of TP5 (a), TP10 (b), and TP11 (c) obtained by LC-QTOF-MS/MS and tentative fragment ion structures

to the presence of alcoholic and carbonylic groups. An additional stepwise elimination of H₂O and CO was also observed, which gave rise to the fragments m/z 188.0281

and 178.0426. This resulted in being the preferential fragmentation pathway. The presence of N₃S in most of the fragments confirmed the integrity of the thiazole and

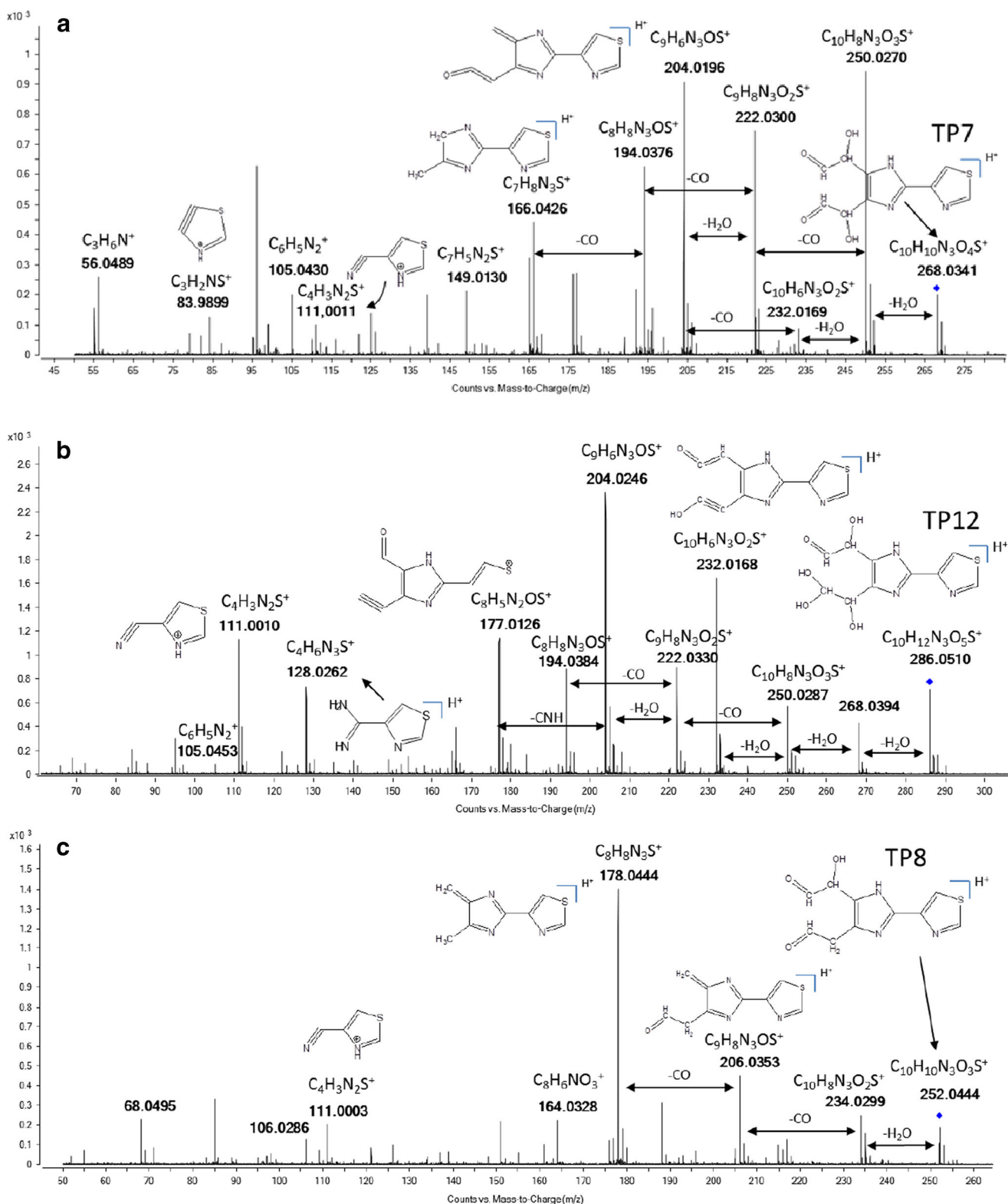


Fig. 6 Product ion spectra of TP7 (a), TP12 (b), and TP8 (c) obtained by LC-QTOF-MS/MS and tentative fragment ion structures

imidazole rings and supported the benzene ring opening theory. Further opening of the imidazole ring is proved by the ion fragment at m/z 111.001 ($C_4H_3N_2S$) also present in other TPs already commented.

TP7 (m/z 268.0384, $C_{10}H_{10}N_3O_4S$) arose from the oxidation of one alcoholic group in TP11, evidenced by the reduction of two hydrogen atoms in the molecular formula with respect to TP11. The protonated

molecular ion loses a water molecule with the formation of m/z 250. A further loss of water leads to the formation of fragment at m/z 232. Subsequently, both ions lose two CO groups (m/z 222 and 204) each. In addition to these stepwise eliminations of H₂O and CO, many others occur simultaneously, resulting in a very complex spectrum (Fig. 6a).

TP12 (m/z 286.0493, C₁₀H₁₂N₃O₅S) was the intermediate displaying a higher grade of oxidation with five oxygen atoms in the structure. Its elemental composition and DBE value reveals the presence of an additional hydroxyl group with respect to TP11 structure. The proposal is the formation of 2-hydroxy-2-(4-(1,2,2-trihydroxyethyl)-2-(thiazol-4-yl)-1H-imidazol-5-yl)acetaldehyde, 2-hydroxy-2-(4-(1,2,2-trihydroxyethyl)-2-(thiazol-4-yl)-1H-imidazol-5-yl)acetaldehyde, since the presence of ions at m/z 178.0426 and 111.001 (Fig. 6b) discards the possibility that the new OH group can occupy positions in the imidazole or thiazole rings. The fragmentation pattern shows three consecutive losses of H₂O (ions at m/z 268, C₁₀H₁₀N₃O₄S; m/z 250, C₁₀H₈N₃O₃S; and m/z 232, C₁₀H₆N₃O₂S), which are consistent with the presence of multiple OH groups. Tentative assignments of the structures of some fragment ions are depicted in Fig. 6b to support the proposed structure of the parent compound.

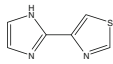
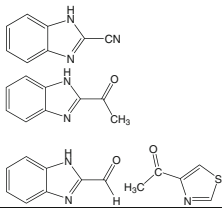
TP8 (m/z 252.0438, C₁₀H₁₀N₃O₃S), showed the same DBE value as TP7, pointing out the presence of two

carbonyl groups in the molecule. However, the number of oxygen atoms was lower, indicating the presence of only one OH group. This was confirmed by the fragmentation pattern that showed only one loss of water (m/z 234) followed by two consecutive CO losses (m/z 206 and 178) (Fig. 6c).

Proposed transformation pathway and evolution profile of TPs

On the basis of the results presented above and taking into account previous studies on the TBZ oxidation (Table 2), two competing pathways (Fig. 7) can be proposed. One is initiated by the addition of the OH to the benzene ring by electrophilic substitution of one hydrogen atom, to bring about the formation of two mono-hydroxylated species (TP2/TP3). No further hydroxylation reactions conducting to poly-hydroxylated derivatives were observed, thus suggesting that further attack of OH on the benzene moiety will ideally lead to ring opening (compounds TP7, TP8, TP11, and TP12). This reaction route had been previously reported by Calza et al. [23] during TiO₂ photocatalysis of TBZ (see Table 2). In this case, structures of TP7 and TP11 were also proposed. In addition, Calza et al. [23] reported the formation of 2-(thiazol-4-yl)-1H-imidazole, not detected under the conditions used in our study. This compound, shown in brackets in Fig. 7, arises as a

Table 2 Summary of previous works concerning TBZ degradation in water

| TPs identified | Treatment applied | Matrix | Irradiation conditions | Analytical conditions | Ref. |
|---|----------------------|---|---|-----------------------------|------|
| TP2/ TP3, TP11, TP6, TP7  | TiO ₂ /UV | Distilled water (15 mg L ⁻¹) | 1500 W xenon lamp (Solarbox) simulating AM1 solar light and equipped with a 340 nm cut-off filter | LC-(APCI)IT-MS ⁿ | [23] |
| TP2/ TP3, TP6, TP10 | Fenton | Distilled water (100 µg L ⁻¹) | — | LC-(ESI)QTOF-MS/MS | [2] |
| TP1, TP5, TP6  | UV | Distilled water (2 mg L ⁻¹) | High pressure mercury lamp (HPK 125W, Philips) λ ≥ 290 nm. | GC-(ED)Q-MS | [22] |

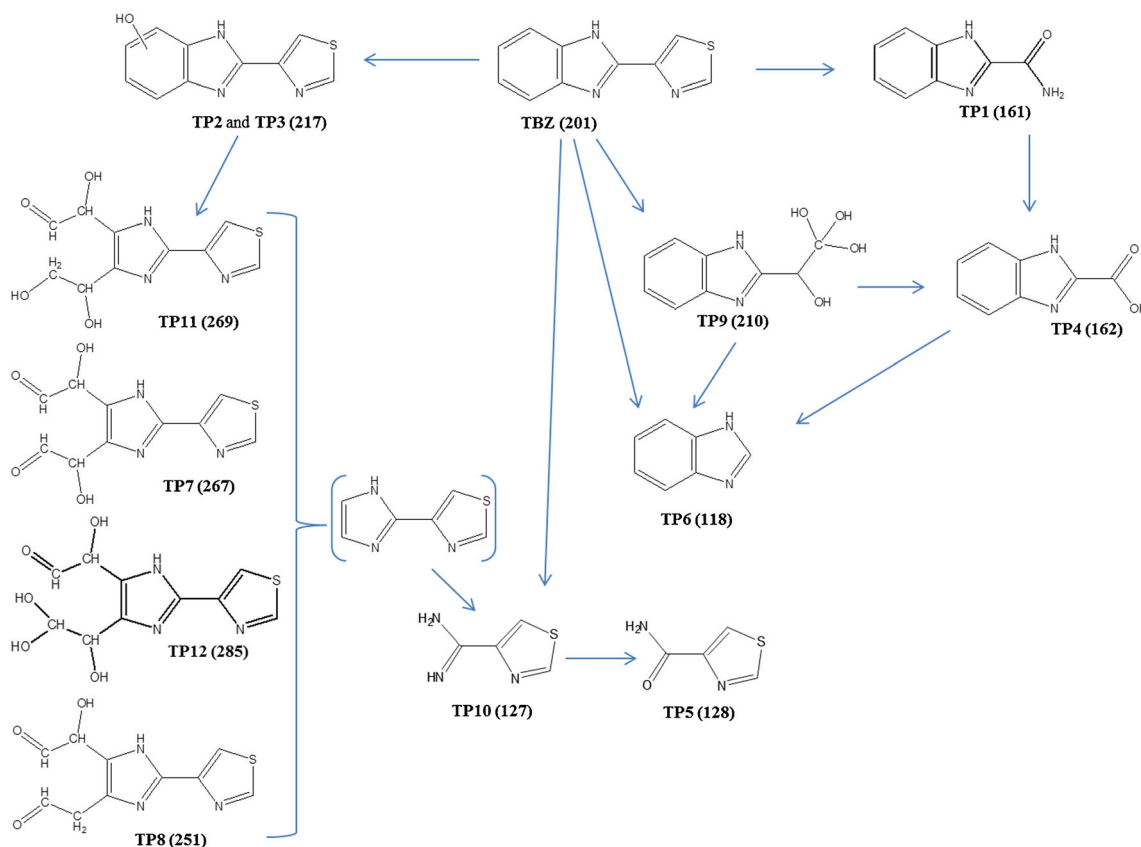


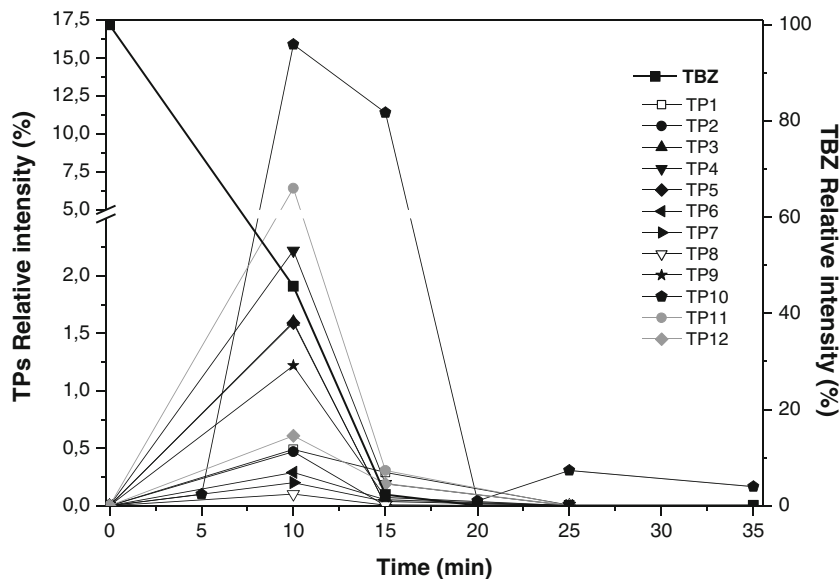
Fig. 7 Tentative transformation pathway of TBZ degradation by the Fenton process

consequence of cleavage of the aliphatic chains and can be considered to be an intermediate step in the formation of TP10 and its subsequent oxidized derivative TP5. These two compounds could also appear as a result of direct breakage of the TBZ molecule by the two N atoms in imidazole ring as proposed by Ji et al. [27] in their study about degradation of the sunscreen agent 2-phenylbenzimidazole-5-sulfonic acid

by TiO₂ photocatalysis. These authors suggest these sites as likely to be attacked by HO radicals due to their high electron density.

A common characteristic of all these compounds was the presence of the thiazole ring in the molecule. However, a concomitant pathway was observed that includes the 'OH attack on this moiety. TP1, TP4, TP6, and TP9 arise as a result

Fig. 8 Relative abundance of the TPs with respect to TBZ during the Fenton treatment



of this reaction. This route had been proposed by Murthy et al. [22] during the photolysis of thiabendazole in aqueous solution, with the identification of TP1 and TP6. Formation of benzimidazole (TP6) is also widely referenced. In the words of Calza et al. [23], this structure is formed through an OH radical attack on the C1' and the consequent C–C chain broken. However, the presence of the benzimidazole moiety in TP1, TP4, and TP9 suggests that these compounds can also arise after the loss of the aliphatic chain.

Figure 8 shows the transformation profile of TBZ and TPs throughout the Fenton treatment. To facilitate the observation, the intensity of the TPs was normalized to the maximum peak intensity of TBZ recorded. All the TPs identified reached maximum intensity after the second iron addition. After that, they all decreased and disappeared, with the exception of TP10 (thiazole-4-carboxamide), which remained even after total elimination of TBZ, thus evidencing the higher stability of the thiazole ring. The highest intensity reached by TP10, even in the early stages of treatment, reinforces the hypothesis that it can be generated from direct breakage of the TBZ molecule [28]. Similarly, the higher intensity reached by TP1, TP4, and TP9 and the fact that the corresponding thiazole moiety was not detected point out the opening of thiazole structure and subsequent losses in the aliphatic chain as the preferred route for the formation of benzimidazol.

Conclusions

TBZ degradation by the Fenton reaction has been assessed through identification of transformation products generated in the process. Two main pathways have been identified that lead to the transformation of this pesticide in water solution. Both initiate with typical hydroxylation reactions which, as a consequence of electrophilic nature of hydroxyl radicals, can occur in both benzimidazole and thiazole rings. LC-QTOF-MS/MS use, along with the experimental conditions selected for the experiments, has allowed up to 12 intermediates to be identified, some of them previously unreported, which increases the available knowledge about the behavior of this compound. Identification of thiazole-4-carboxamide in the last stage of the treatment again represents evidence for the necessity of monitoring both parents and TPs. The identification of these TPs will help in the implementation of more complete analytical methods where the presence of TPs could be evaluated in a joint analysis of reference compounds in environmental samples (surface water and sediment).

Acknowledgments This research was supported by the Ministry of Economy and Competitiveness (FOTOREG, CTQ 2010-20740-C03-01/PPQ and CTQ 2010-20740-C03-03/PPQ) and the European Regional Development Fund (ERDF). Irene Carra would like to acknowledge the Ministry of Education, Culture and Sport for her FPU scholarship (AP2010-3218).

References

- Köck-Schulmeyer M, Villagrasa M, de Alda ML, Céspedes-Sánchez R, Ventura F, Barceló D (2013) Occurrence and behavior of pesticides in wastewater treatment plants and their environmental impact. *Sci Total Environ* 458–460:466–476
- Peréz JAS, Carra I, Sirtori C, Agüera A, Esteban B (2014) Fate of thiabendazole through the treatment of a simulated agro-food industrial effluent by combined MBR/Fenton processes at $\mu\text{g/L}$ scale. *Water Res* 51:55–63
- Veneziano A, Vacca G, Arana S, de Simone F, Rastrelli L (2004) Determination of carbendazim, thiabendazole and thiophanate-methyl in banana (*Musa acuminata*) samples imported to Italy. *Food Chem* 87:383–386
- Castillo LE, Ruepert C, Solis E (2000) Pesticide residues in the aquatic environment of banana plantation: areas in the north Atlantic zone of Costa Rica. *Environ Toxicol Chem* 19:1942–1950
- Müller C, David L, Chiş V, Pînzaru SC (2014) Detection of thiabendazole applied on citrus fruits and bananas using surface enhanced Raman scattering. *Food Chem* 145:814–820
- Ito Y, Ikai Y, Oka H, Hayakawa J, Kagami T (1998) Application of ion-exchange cartridge clean-up in food analysis: I. Simultaneous determination of thiabendazole and imazalil in citrus fruit and banana using high-performance liquid chromatography with ultraviolet detection. *J Chromatogr A* 810:81–87
- Cuadros S, Manresa MÀ, Font J, Bautista ME, Puig R, Marsal A (2012) Alternative fungicides for the leather industry: application in various processes. *J Soc Leath Tech Ch* 96:225–233
- Karas PA, Perruchon C, Exarhou K, Ehaliotis C, Karpouzas DG (2011) Potential for bioremediation of agro-industrial effluents with high loads of pesticides by selected fungi. *Biodegradation* 22:215–228
- Bernabeu A, Vercher RF, Santos-Juanes L, Simón PJ, Lardín C, Martínez MA, Vicente JA, González R, Llosá C, Arques A, Amat AM (2011) Solar photocatalysis as a tertiary treatment to remove emerging pollutants from wastewater treatment plant effluents. *Catal Today* 161:235–240
- Sievers M (2011) Advanced oxidation processes. *Treatise on Water Science* 4:377–408
- Klamerth N, Malato S, Agüera A, Fernández-Alba A (2013) Photo-Fenton and modified photo-Fenton at neutral pH for the treatment of emerging contaminants in wastewater treatment plant effluents: a comparison. *Water Res* 47:833–840
- Klamerth N, Rizzo L, Malato S, Maldonado MI, Agüera A, Fernández-Alba AR (2010) Degradation of fifteen emerging contaminants at μgL^{-1} initial concentrations by mild solar photo-Fenton in MWTP effluents. *Water Res* 44:545–554
- Klamerth N, Malato S, Maldonado MI, Agüera A, Fernández-Alba A (2011) Modified photo-Fenton for degradation of emerging contaminants in municipal wastewater effluents. *Catal Today* 161:241–246
- Trovó AG, Nogueira RFP, Agüera A, Fernández-Alba AR, Sirtori C, Malato S (2009) Degradation of sulfamethoxazole in water by solar photo-Fenton. Chemical and toxicological evaluation. *Water Res* 43:3922–3931
- Fatta-Kassinos D, Kalavrouziotis IK, Koukoulakis PH, Vasquez MI (2011) The risks associated with wastewater reuse and xenobiotics in the agroecological environment. *Sci Total Environ* 409:3555–3563
- Sirtori C, Agüera A, Gemjak W, Malato S (2010) Effect of water-matrix composition on Trimethoprim solar photodegradation kinetics and pathways. *Water Res* 44:2735–2744
- Agüera A, Bueno MJM, Fernández-Alba AR (2013) New trends in the analytical determination of emerging contaminants and their transformation products in environmental waters. *Environ Sci Pollut R* 20:3496–3515

18. Lam MW, Mabury SA (2005) Photodegradation of the pharmaceuticals atorvastatin, carbamazepine, levofloxacin, and sulfamethoxazole in natural waters. *Aquat Sci* 67:177–188
19. Malato S, Albanis T, Piedra L, Agüera A, Hernando D, Fernández-Alba A (2003) In: Ferrer I, Thurman EM (eds) *Liquid chromatography/mass spectrometry, MS/MS and time-of-flight MS analysis of emerging contaminants*. American Chemical Society, Washington
20. Agüera A, Gómez-Ramos MM, Fernández-Alba AR (2012) In: Fernández-Alba AR (ed) *TOF-MS within food and environmental analysis*. Elsevier, Amsterdam
21. Watkins DAM (1976) Photolysis of thiabendazole. *Chemosphere* 5: 77–78
22. Moza PN, Murthy NBK, Hustert K, Raghu K, Kettrup A (1996) Photolysis of thiabendazole in aqueous solution and in the presence of fulvic and humic acids. *Chemosphere* 33: 1915–1920
23. Calza P, Baudino S, Aigotti R, Baiocchi C, Pelizzetti E (2003) Ion trap tandem mass spectrometric identification of thiabendazole phototransformation products on titanium dioxide. *J Chromatogr A* 984:59–66
24. Nogueira RFP, Oliveira MC, Paterlini WC (2005) Simple and fast spectrophotometric determination of H₂O₂ in photo-Fenton reactions using metavanadate. *Talanta* 66:86–91
25. Ikehata K, El-Din MG (2006) Aqueous pesticide degradation by hydrogen peroxide/ultraviolet irradiation and Fenton-type advanced oxidation processes: a review. *J Environ Eng Sci* 5:81–135
26. Pignatello JJ, Oliveros E, MacKay A (2006) Advanced oxidation processes for organic contaminant destruction based on the Fenton reaction and related chemistry. *Crit Rev Env Sci Technol* 36:1–84
27. Ji Y, Zhou L, Ferronato C, Salvador A, Yang X (2013) Degradation of sunscreen agent 2-phenylbenzimidazole-5-sulfonic acid by TiO₂ photocatalysis: kinetics, photoproducts and comparison to structurally related compounds. *Appl Catal B* 140–141:457–467
28. Fujitani T, Yoneyama M, Ogata A, Ueta T, Mori K, Ichikawa H (1991) New metabolites of thiabendazole and the metabolism of thiabendazole by mouse embryo in vivo and in vitro. *Food Chem Toxicol* 29:265–274